Optimal feedback mechanisms for regulating cell numbers

Saurabh Modi[1], and Abhyudai Singh[1,2,3,*]

1. Department of Biomedical Engineering, University of Delaware, Newark, DE, USA.

2. Department of Electrical and Computer Engineering, University of Delaware, Newark, DE, USA.

3. Department of Mathematical Sciences, University of Delaware, Newark, DE, USA.

* Corresponding Author: Abhyudai Singh, absingh@udel.edu.

Abstract

How living cells employ counting mechanisms to regulate their numbers or density is a long-standing problem in developmental biology that ties directly with organism or tissue size. Diverse cells types have been shown to regulate their numbers via secretion of factors in the extracellular space. These factors act as a proxy for the number of cells and function to reduce cellular proliferation rates creating a negative feedback. It is desirable that the production rate of such factors be kept as low as possible to minimize energy costs and detection by predators. Here we formulate a stochastic model of cell proliferation with feedback control via a secreted extracellular factor. Our results show that while low levels of feedback minimizes random fluctuations in cell numbers around a given set point, high levels of feedback amplify Poisson fluctuations in secreted-factor copy numbers. This trade-off results in an optimal feedback strength, and sets a fundamental limit to noise suppression in cell numbers. Intriguingly, this fundamental limit depends additively on two variables: relative half-life of the secreted factor with respect to the cell proliferation rate, and the average number of factors secreted in a cell's lifespan. We further expand the model to consider external disturbances in key physiological parameters, such as, proliferation and factor synthesis rates. Intriguingly, while negative feedback effectively mitigates disturbances in the proliferation rate, it amplifies disturbances in the synthesis rate. In summary, these results provide unique insights into the functioning of feedback-based counting mechanisms, and apply to organisms ranging from unicellular prokaryotes and eukaryotes to human cells.

1 Introduction

In order to achieve physiological function various animals regulate their morphology [1]. For example, tissue size may be regulated by either controlling the sizes of individual cells, or the number of constituent cells [2–6]. How individual cells maintain size homeostasis has been extensively studied across organisms ranging from bacteria, animal and plant cells [7–16]. Interestingly, data reveals cell-autonomous control strategies that regulate cellular growth or timing of cell-cycle events to suppress aberrant deviations in cell size around an optimal size specific to that cell type [17–20]. In contrast, mechanisms that control cell numbers have been less understood.

One strategy to control cell numbers is for cells to secrete a molecule that accumulates in the extracellular space, and is sensed by other cells in the population [21–23]. Binding of this secreted factor to cell surface receptors activates signaling pathway that inhibit cell proliferation, thus creating a negative feedback loop (Fig. 1). Such feedback control via secreted factors has been reported in many organisms including *Myxococcus xanthus* [24], *Vibrio fischeri* [25], *Bacillus subtilis* [26], *Dictyostelium discoideum* [27, 28], multicellular animals [29, 30] and plants [31]. For illustration purposes, we show some published data on *Dictyostelium discoideum* in Fig. 1, where the proliferation rates decrease monotonically with increasing buildup of the secreted factor.

The feedback strategy illustrated in Fig. 1 creates an interesting tradeoff, where cells incur a cost to produce the factor and would prefer to keep its synthesis to as low as possible. However, a side effect of low levels is shot noise or Poisson fluctuations in secreted factor copy numbers that are propagated to cell numbers. Here we study this tradeoff through a mathematical model that incorporates three different noise mechanisms: stochastic proliferation of cells; stochastic synthesis of the secreted factor from single cells; and external disturbances in model parameters. Our analysis reveals that depending on the source of noise, negative feedback can either buffer or amplify random fluctuations in cell numbers around a given set point. Moreover, when multiple noise sources are present, then an optimal feedback strength provides the most efficient noise buffering. This optimal feedback sets up a fundamental lower limit for minimizing fluctuations in cell numbers, and we systematically study how this limit scales with different parameters. We start by formally introducing the mathematical model followed by its stochastic analysis.

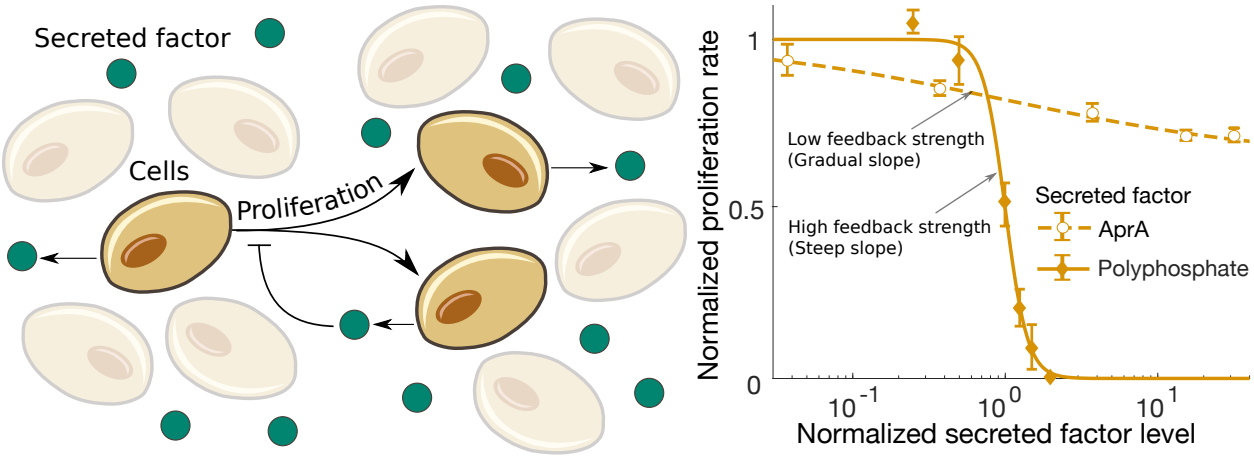

Figure 1: **Controlling cell numbers by feedback control through secreted extracellular factors.** *Left.* Schematic of a cell population, where each cell proliferates and secretes a molecule in the extracellular space. The buildup of secreted factors is sensed by other cells in the population. The factor functions to inhibit cell proliferation creating homeostasis in cell numbers. *Right.* Data showing proliferation rates of *Dictyostelium discoideum* cells with respect to the levels of two different secreted factors (*AprA* and *Polyphosphate*) . While the inhibition of proliferation rate by *AprA* is gradual, that by *Polyphosphate* is relatively steep and occurs over a narrower range of factor levels. The error bars are the standard errors corresponding to the raw data, and lines represent Hill equations fitted to the data. We refer the reader to [32, 33] for further biological details and experimental procedures.

2 Stochastic model formulation

Let $\boldsymbol{x}(t)$ and $\boldsymbol{z}(t)$ denote the number of cells, and the number of secreted factors at time t, respectively. Cells are assumed to proliferate exponentially with a rate $g(\boldsymbol{z})$, with g being a monotonically decreasing function as illustrated in Fig. 1. Moreover, cells are removed (or die) from the population at a rate $\gamma_{\boldsymbol{x}}$. Finally, each cell synthesizes and secretes the factor at a rate $k_{\boldsymbol{z}}$, and these secreted factors decay with a rate $\gamma_{\boldsymbol{z}}$. The stochastic formation of this model is shown in Table 1 and consists of four probabilistic events that increase/decrease the population counts by one. The propensity functions in the last column determine how often the events occur. For example, the propensity function for the cell proliferation event is $g(\boldsymbol{z})\,\boldsymbol{x}$ which implies that the probability this event will occur in the next time interval $(t, t+dt)$ is $g(\boldsymbol{z})\,\boldsymbol{x}dt$, and whenever the event occurs the cell count increases by one.

Throughout the paper we denote by $\langle \boldsymbol{x}(t) \rangle$ as the mean value of the stochastic process $\boldsymbol{x}(t)$, and by $\overline{\langle \boldsymbol{x} \rangle} = \lim_{t\to\infty} \langle \boldsymbol{x}(t) \rangle$ its steady-state value. Based on the stochastic model in Table 1, the population

averages evolve as

$$\frac{d\langle \boldsymbol{z} \rangle}{dt} = k_{\boldsymbol{z}} \langle \boldsymbol{x} \rangle - \gamma_{\boldsymbol{z}} \langle \boldsymbol{z} \rangle \tag{1}$$

$$\frac{d\langle \boldsymbol{x} \rangle}{dt} = \langle \boldsymbol{x} g\left(\boldsymbol{z}\right) \rangle - \gamma_{\boldsymbol{x}} \langle \boldsymbol{x} \rangle \tag{2}$$

[34, 35]. In the deterministic mean-field limit where

$$\langle \boldsymbol{x} g\left(\boldsymbol{z}\right) \rangle \approx \langle \boldsymbol{x} \rangle g\left(\langle \boldsymbol{z} \rangle\right) \tag{3}$$

we obtain the following approximated nonlinear system

$$\frac{d\langle \boldsymbol{z} \rangle}{dt} = k_{\boldsymbol{z}} \langle \boldsymbol{x} \rangle - \gamma_{\boldsymbol{z}} \langle \boldsymbol{z} \rangle \tag{4}$$

$$\frac{d\langle \boldsymbol{x} \rangle}{dt} = \langle \boldsymbol{x} \rangle g\left(\langle \boldsymbol{z} \rangle\right) - \gamma_{\boldsymbol{x}} \langle \boldsymbol{x} \rangle \tag{5}$$

that has a unique equilibrium defined by the solution to the equations

$$g\left(\overline{\langle \boldsymbol{z} \rangle}\right) = \gamma_{\boldsymbol{x}}, \;\; \overline{\langle \boldsymbol{x} \rangle} = \frac{\gamma_{\boldsymbol{z}} \overline{\langle \boldsymbol{z} \rangle}}{k_{\boldsymbol{z}}} \tag{6}$$

as long as $g\left(0\right) > \gamma_{\boldsymbol{x}} > g\left(\infty\right)$. Having determined the mean equilibrium population counts, we next quantify the negative feedback strength by the dimensionless parameter

$$f := -\frac{\overline{\langle \boldsymbol{z} \rangle} g'(\overline{\langle \boldsymbol{z} \rangle})}{g\left(\overline{\langle \boldsymbol{z} \rangle}\right)} > 0 \tag{7}$$

that is essentially the log sensitivity of g at $\boldsymbol{z} = \overline{\langle \boldsymbol{z} \rangle}$. Local stability analysis of the equilibrium point yields the following eigenvalues of the linearized system

$$\frac{-\gamma_{\boldsymbol{z}} \pm \sqrt{\gamma_{\boldsymbol{z}}^2 - 4 f \gamma_{\boldsymbol{x}} \gamma_{\boldsymbol{z}}}}{2} \tag{8}$$

and shows that the equilibrium of the nonlinear system (4)-(5) is stable for $f > 0$. Note that sufficiently strong negative feedback ($f > \gamma_{\boldsymbol{z}}/4\gamma_{\boldsymbol{x}}$) results in complex eigenvalues with negative real parts, and in this case as the noise kicks the system out of equilibrium, the relaxation dynamics will be oscillatory.

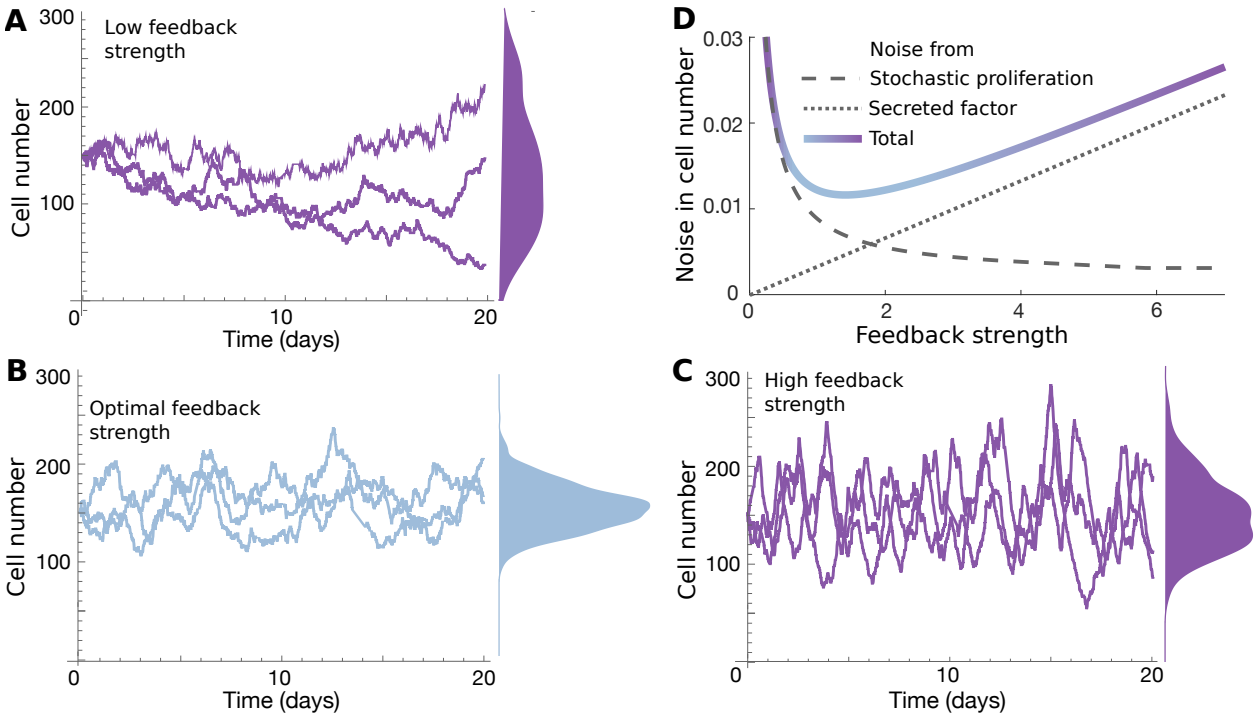

Figure 2: **Noise in cell numbers is minimized at an intermediate level of negative feedback.** Stochastic simulation of the model presented in Table 1 using [36] for different feedback strengths A.$f = 0.01$ (Low), B. $f = 0.6$ (Optimal), C. $f = 10$ (High). For a given mean number of cells, the spread in cell numbers first reduces, and then increases with increasing feedback strength. D. Plotting the total noise, and the different noise components in (16) as a function of f. While the noise contribution from stochastic proliferation reduces, the contribution from stochastic secreted-factor synthesis and decay increases creating a U-shape profile of the total noise. Parameters chosen for all the above subfigures were: $\gamma_{\boldsymbol{z}} = 3\gamma_{\boldsymbol{x}} = 3\ day^{-1}, \overline{\langle \boldsymbol{z} \rangle} = 100, \overline{\langle \boldsymbol{x} \rangle} = 150$.

Table 1: Stochastic model of cell proliferation and feedback inhibition via secreted factors.

Probabilistic event	Change in population counts	Propensity function
Cell proliferation	$\boldsymbol{x}(t) \mapsto \boldsymbol{x}(t)+1$	$g\left(\boldsymbol{z}(t)\right)\boldsymbol{x}(t)$
Cell death	$\boldsymbol{x}(t) \mapsto \boldsymbol{x}(t)-1$	$\gamma_{\boldsymbol{x}}\boldsymbol{x}(t)$
Secreted factor synthesis	$\boldsymbol{z}(t) \mapsto \boldsymbol{z}(t)+1$	$k_{\boldsymbol{z}}\boldsymbol{x}(t)$
Secreted factor degradation	$\boldsymbol{z}(t) \mapsto \boldsymbol{z}(t)-1$	$\gamma_{\boldsymbol{z}}\boldsymbol{z}(t)$

3 Optimal feedback strength for regulating cell numbers

A stochastic simulation of the feedback system via the Gillespie algorithm reveals an intriguing feature - while low levels of feedback strength attenuate random fluctuations in cell numbers, a strong negative feedback amplifies fluctuations (Fig. 2). We further investigate this effect by developing approximate analytical formulas for the noise in cell numbers, where noise is quantified by the steady-state coefficient of variation of $\boldsymbol{x}(t)$. A well-known problem that often arises when dealing with nonlinear stochastic systems is unclosed moment dynamics - time evolution of lower order moments depends on higher order moments [37]. While a number of closure methods have been developed to tackle this issue [38–51], we circumvent this problem by exploiting the Linear Noise Approximation (LNA) [52]. Assuming small fluctuations in $\boldsymbol{x}(t)$ and $\boldsymbol{z}(t)$ around their respective steady-state means, LNA works by linearizing the nonlinear propensity functions

$$\boldsymbol{x}g\left(\boldsymbol{z}\right) \approx g\left(\overline{\langle \boldsymbol{z} \rangle}\right)\left(\boldsymbol{x} - f\overline{\langle \boldsymbol{x} \rangle}\frac{\boldsymbol{z}-\overline{\langle \boldsymbol{z} \rangle}}{\overline{\langle \boldsymbol{z} \rangle}}\right), \tag{9}$$

and with this approximation all propensity functions in Table 1 are now linear functions of the state space. Time evolution of statistical moments is obtained using the following result from our prior work [35, 37]: the time derivative of the expected value of an arbitrary function $\psi(\boldsymbol{x},\boldsymbol{z})$ is given by

$$\begin{aligned}\frac{d\langle\psi(\boldsymbol{x},\boldsymbol{z})\rangle}{dt} &= \langle k_{\boldsymbol{z}}\boldsymbol{x}[\psi(\boldsymbol{x},\boldsymbol{z}+1)-\psi(\boldsymbol{x},\boldsymbol{z})]\rangle + \langle g\left(\overline{\langle \boldsymbol{z} \rangle}\right)\overline{\langle \boldsymbol{x} \rangle}\left(\frac{\boldsymbol{x}}{\overline{\langle \boldsymbol{x} \rangle}} - f\frac{\boldsymbol{z}-\overline{\langle \boldsymbol{z} \rangle}}{\overline{\langle \boldsymbol{z} \rangle}}\right)[\psi(\boldsymbol{x}+1,\boldsymbol{z})-\psi(\boldsymbol{x},\boldsymbol{z})]\rangle \\ &+ \langle \gamma_{\boldsymbol{x}}\boldsymbol{x}[\psi(\boldsymbol{x}-1,\boldsymbol{z})-\psi(\boldsymbol{x},\boldsymbol{z})]\rangle + \langle \gamma_{\boldsymbol{z}}\boldsymbol{z}[\psi(\boldsymbol{x},\boldsymbol{z}-1)-\psi(\boldsymbol{x},\boldsymbol{z})]\rangle. \end{aligned} \tag{10}$$

Substituting appropriate monomials for $\psi(\boldsymbol{x}, \boldsymbol{z})$ above yields the following system of differential equations for all the first and second order moments of $\boldsymbol{x}(t)$ and $\boldsymbol{z}(t)$

$$\frac{d\langle \boldsymbol{x} \rangle}{dt} = g\left(\overline{\langle \boldsymbol{z} \rangle}\right) \overline{\langle \boldsymbol{x} \rangle} \left(\frac{\langle \boldsymbol{x} \rangle}{\overline{\langle \boldsymbol{x} \rangle}} - f \frac{\langle \boldsymbol{z} \rangle - \overline{\langle \boldsymbol{z} \rangle}}{\overline{\langle \boldsymbol{z} \rangle}} \right) - \gamma_{\boldsymbol{x}} \langle \boldsymbol{x} \rangle \tag{11}$$

$$\frac{d\langle \boldsymbol{z} \rangle}{dt} = k_{\boldsymbol{z}} \langle \boldsymbol{x} \rangle - \gamma_{\boldsymbol{z}} \langle \boldsymbol{z} \rangle \tag{12}$$

$$\frac{d\langle \boldsymbol{x}\boldsymbol{z} \rangle}{dt} = g\left(\overline{\langle \boldsymbol{z} \rangle}\right) \overline{\langle \boldsymbol{x} \rangle} \left(\frac{\langle \boldsymbol{x}\boldsymbol{z} \rangle}{\overline{\langle \boldsymbol{x} \rangle}} - f \frac{\langle \boldsymbol{z}^2 \rangle - \overline{\langle \boldsymbol{z} \rangle} \langle \boldsymbol{z} \rangle}{\overline{\langle \boldsymbol{z} \rangle}} \right) + k_{\boldsymbol{z}} \langle \boldsymbol{x}^2 \rangle - (\gamma_{\boldsymbol{x}} + \gamma_{\boldsymbol{z}}) \langle \boldsymbol{x}\boldsymbol{z} \rangle \tag{13}$$

$$\frac{d\langle \boldsymbol{x}^2 \rangle}{dt} = \gamma_{\boldsymbol{x}} (\langle \boldsymbol{x} \rangle - 2\langle \boldsymbol{x}^2 \rangle) + g\left(\overline{\langle \boldsymbol{z} \rangle}\right) \overline{\langle \boldsymbol{x} \rangle} \left(\frac{\langle \boldsymbol{x} \rangle}{\overline{\langle \boldsymbol{x} \rangle}} - f \frac{\langle \boldsymbol{z} \rangle - \overline{\langle \boldsymbol{z} \rangle}}{\overline{\langle \boldsymbol{z} \rangle}} \right) + 2g\left(\overline{\langle \boldsymbol{z} \rangle}\right) \overline{\langle \boldsymbol{x} \rangle} \left(\frac{\langle \boldsymbol{x}^2 \rangle}{\overline{\langle \boldsymbol{x} \rangle}} - f \frac{\langle \boldsymbol{x}\boldsymbol{z} \rangle - \langle \boldsymbol{x} \rangle \overline{\langle \boldsymbol{z} \rangle}}{\overline{\langle \boldsymbol{z} \rangle}} \right) \tag{14}$$

$$\frac{d\langle \boldsymbol{z}^2 \rangle}{dt} = \gamma_{\boldsymbol{z}} (\langle \boldsymbol{z} \rangle - 2\langle \boldsymbol{z}^2 \rangle) + k_{\boldsymbol{z}} \langle \boldsymbol{x} \rangle + 2k_{\boldsymbol{z}} \langle \boldsymbol{x}\boldsymbol{z} \rangle. \tag{15}$$

Solving the moment equations at steady state we obtain the following noise (coefficient of variation squared) in cell numbers

$$CV_{\boldsymbol{x}}^2 = \underbrace{\frac{\gamma_{\boldsymbol{x}} f}{\gamma_{\boldsymbol{z}} \overline{\langle \boldsymbol{z} \rangle}}}_{\substack{\text{Noise from} \\ \text{secreted factor}}} + \underbrace{\frac{\gamma_{\boldsymbol{z}} + \gamma_{\boldsymbol{x}} f}{\gamma_{\boldsymbol{z}} f \overline{\langle \boldsymbol{x} \rangle}}}_{\substack{\text{Noise from} \\ \text{stochastic proliferation}}} \tag{16}$$

which can be decomposed into two terms. The first term represents the noise contribution from Poisson fluctuations in $\boldsymbol{z}(t)$ (noise from secreted factor) and the other term is the contribution from stochastic proliferation/death of cells. Note that $CV_{\boldsymbol{x}}$ decreases as the secreted factor half-life decreases, which makes intuitive sense as then the regulator tracks the cell numbers more faithfully. Interestingly, the first term is amplified, and second term is attenuated with increasing feedback strength f (Fig. 2). These opposing effects result in $CV_{\boldsymbol{x}}^2$ being minimized at an optimal feedback strength

$$f = \frac{\sqrt{\gamma_{\boldsymbol{z}} \overline{\langle \boldsymbol{z} \rangle}}}{\sqrt{\gamma_{\boldsymbol{x}} \overline{\langle \boldsymbol{x} \rangle}}}. \tag{17}$$

Replacing (17) in (16) and using (3) yields the fundamental limit of noise suppression in cell numbers as

$$CV_{\boldsymbol{x}}^2 = \frac{\frac{\gamma_{\boldsymbol{x}}}{\gamma_{\boldsymbol{z}}} + \frac{2\sqrt{\gamma_{\boldsymbol{x}}}}{\sqrt{k_{\boldsymbol{z}}}}}{\overline{\langle \boldsymbol{x} \rangle}}. \tag{18}$$

While inverse scaling of $CV_{\boldsymbol{x}}^2$ with respect to the mean $\overline{\langle \boldsymbol{x} \rangle}$ is reminiscent of Poisson-like fluctuations, the numerator value can be made small by having a short-lived secreted factor (high $\gamma_{\boldsymbol{z}}$) *and* a high factor synthesis rate $k_{\boldsymbol{z}}$. It is interesting to point out that the ratio $N = k_{\boldsymbol{z}}/\gamma_{\boldsymbol{x}}$ is the average number of secreted factors made by an individual cell in its lifespan, and the fundamental noise limit scales as $1/\sqrt{N}$, but the scaling is $1/\gamma_{\boldsymbol{z}}$ with respect to the factor decay rate.

4 Incorporating external disturbances in physiological parameters

Our analysis up till now assume constant model parameters, and we now expand the model to allow for external disturbances that transform parameters into stochastic processes.

4.1 External disturbance in the proliferation rate

Data shows that the cellular growth rate can randomly fluctuate with some memory over many generations [53–57], and its not hard to imagine these features carrying over to the cell proliferation rate. Motivated by these findings we assume that the proliferation rate $g\left(\boldsymbol{z}, \boldsymbol{y}\right)$ is affected by an external factor $\boldsymbol{y}$ whose stochastic dynamics is modeled as an Ornstein-Uhlenbeck process

$$d\boldsymbol{y}(t) = \gamma_{\boldsymbol{y}}(\overline{\langle \boldsymbol{y} \rangle} - \boldsymbol{y}(t))dt + \sigma_{\boldsymbol{y}} d\boldsymbol{w}(t). \tag{19}$$

Here, $\overline{\langle \boldsymbol{y} \rangle}$ is the mean level of external disturbance, $\boldsymbol{w}(t)$ is the Wiener process, $\sigma_{\boldsymbol{y}}$ and $\gamma_{\boldsymbol{y}}$ are parameters that represent the strength of noise and the time-scale of fluctuations in $\boldsymbol{y}$, respectively. Linearizing the proliferation rate

$$\boldsymbol{x} g\left(\boldsymbol{z}, \boldsymbol{y}\right) \approx \overline{\langle \boldsymbol{x} \rangle} g\left(\overline{\langle \boldsymbol{z} \rangle}, \overline{\langle \boldsymbol{y} \rangle}\right) \left(\frac{\boldsymbol{x}}{\overline{\langle \boldsymbol{x} \rangle}} - f \frac{\boldsymbol{z} - \overline{\langle \boldsymbol{z} \rangle}}{\overline{\langle \boldsymbol{z} \rangle}} + S_{\boldsymbol{x}} \frac{\boldsymbol{y} - \overline{\langle \boldsymbol{y} \rangle}}{\overline{\langle \boldsymbol{y} \rangle}} \right), S_{\boldsymbol{x}} := \frac{\overline{\langle \boldsymbol{y} \rangle}}{g\left(\overline{\langle \boldsymbol{z} \rangle}, \overline{\langle \boldsymbol{y} \rangle}\right)} \frac{\partial g\left(\overline{\langle \boldsymbol{z} \rangle}, y\right)}{\partial y}\Big|_{y=\overline{\langle \boldsymbol{y} \rangle}} \tag{20}$$

where $S_{\boldsymbol{x}}$ is the log sensitivity of the proliferation rate to the external disturbance. With this approximations we again repeat the analysis of obtaining moment equations and solving it to get noise in cell numbers. We write the moment dynamics of an arbitrary function $\psi(\boldsymbol{x}, \boldsymbol{y}, \boldsymbol{z})$ using the following result

$$\frac{d\langle \psi(\boldsymbol{x}, \boldsymbol{y}, \boldsymbol{z}) \rangle}{dt} = \langle (L\psi)(\boldsymbol{x}, \boldsymbol{y}, \boldsymbol{z}) \rangle \tag{21}$$

[34], where

$$(L\psi)(x,y,z) := \frac{\partial\psi(x,y,z)}{\partial y}\gamma_{\boldsymbol{y}}\left(\overline{\langle \boldsymbol{y}\rangle} - y\right) + \frac{1}{2}\left(\frac{\partial^2\psi(x,y,z)}{\partial y^2}\sigma_{\boldsymbol{y}}^2\right) + k_{\boldsymbol{z}}x[\psi(x,y,z+1) - \psi(x,y,z)]$$
$$+ g\left(\overline{\langle \boldsymbol{z}\rangle}, \overline{\langle \boldsymbol{y}\rangle}\right)\overline{\langle \boldsymbol{x}\rangle}\left(\frac{x}{\overline{\langle \boldsymbol{x}\rangle}} - f\frac{z-\overline{\langle \boldsymbol{z}\rangle}}{\overline{\langle \boldsymbol{z}\rangle}} + S_{\boldsymbol{x}}\frac{y-\overline{\langle \boldsymbol{y}\rangle}}{\overline{\langle \boldsymbol{y}\rangle}}\right)[\psi(x+1,y,z) - \psi(x,y,z)]$$
$$+ \gamma_{\boldsymbol{x}}x[\psi(x-1,y,z) - \psi(x,y,z)] + \gamma_{\boldsymbol{z}}z[\psi(x,y,z-1) - \psi(x,y,z)]. \tag{22}$$

Substituting appropriately monomials for $\psi(\boldsymbol{x},\boldsymbol{y},\boldsymbol{z})$ we obtain the following moment dynamics

$$\frac{d\langle \boldsymbol{x}\rangle}{dt} = g\left(\overline{\langle \boldsymbol{z}\rangle}, \overline{\langle \boldsymbol{y}\rangle}\right)\overline{\langle \boldsymbol{x}\rangle}\left(\frac{\langle \boldsymbol{x}\rangle}{\overline{\langle \boldsymbol{x}\rangle}} - f\frac{\langle \boldsymbol{z}\rangle - \overline{\langle \boldsymbol{z}\rangle}}{\overline{\langle \boldsymbol{z}\rangle}} + S_{\boldsymbol{x}}\frac{\langle \boldsymbol{y}\rangle - \overline{\langle \boldsymbol{y}\rangle}}{\overline{\langle \boldsymbol{y}\rangle}}\right) - \gamma_{\boldsymbol{x}}\langle \boldsymbol{x}\rangle \tag{23}$$
$$\frac{d\langle \boldsymbol{z}\rangle}{dt} = k_{\boldsymbol{z}}\langle \boldsymbol{x}\rangle - \gamma_{\boldsymbol{z}}\langle \boldsymbol{z}\rangle \tag{24}$$
$$\frac{d\langle \boldsymbol{y}\rangle}{dt} = \gamma_{\boldsymbol{y}}\left(\overline{\langle \boldsymbol{y}\rangle} - \langle \boldsymbol{y}\rangle\right) \tag{25}$$
$$\frac{d\langle \boldsymbol{xz}\rangle}{dt} = g\left(\overline{\langle \boldsymbol{z}\rangle}, \overline{\langle \boldsymbol{y}\rangle}\right)\overline{\langle \boldsymbol{x}\rangle}\left(\frac{\langle \boldsymbol{xz}\rangle}{\overline{\langle \boldsymbol{x}\rangle}} - f\frac{\langle \boldsymbol{z}^2\rangle - \overline{\langle \boldsymbol{z}\rangle}\langle \boldsymbol{z}\rangle}{\overline{\langle \boldsymbol{z}\rangle}} + S_{\boldsymbol{x}}\frac{\langle \boldsymbol{yz}\rangle - \overline{\langle \boldsymbol{y}\rangle}\langle \boldsymbol{z}\rangle}{\overline{\langle \boldsymbol{y}\rangle}}\right) + k_{\boldsymbol{z}}\langle \boldsymbol{x}^2\rangle - (\gamma_{\boldsymbol{x}} + \gamma_{\boldsymbol{z}})\langle \boldsymbol{xz}\rangle \tag{26}$$
$$\frac{d\langle \boldsymbol{xy}\rangle}{dt} = g\left(\overline{\langle \boldsymbol{z}\rangle}, \overline{\langle \boldsymbol{y}\rangle}\right)\overline{\langle \boldsymbol{x}\rangle}\left(\frac{\langle \boldsymbol{xy}\rangle}{\overline{\langle \boldsymbol{x}\rangle}} - f\frac{\langle \boldsymbol{yz}\rangle - \overline{\langle \boldsymbol{z}\rangle}\langle \boldsymbol{y}\rangle}{\overline{\langle \boldsymbol{z}\rangle}} + S_{\boldsymbol{x}}\frac{\langle \boldsymbol{y}^2\rangle - \overline{\langle \boldsymbol{y}\rangle}\langle \boldsymbol{y}\rangle}{\overline{\langle \boldsymbol{y}\rangle}}\right) + \gamma_{\boldsymbol{y}}\left(\langle \boldsymbol{x}\rangle\overline{\langle \boldsymbol{y}\rangle} - \langle \boldsymbol{xy}\rangle\right)$$
$$- \gamma_{\boldsymbol{x}}\langle \boldsymbol{xy}\rangle \tag{27}$$
$$\frac{d\langle \boldsymbol{yz}\rangle}{dt} = \gamma_{\boldsymbol{y}}(\overline{\langle \boldsymbol{y}\rangle}\langle \boldsymbol{z}\rangle - \langle \boldsymbol{yz}\rangle) + k_{\boldsymbol{z}}\langle \boldsymbol{xy}\rangle - \gamma_{\boldsymbol{z}}\langle \boldsymbol{yz}\rangle \tag{28}$$
$$\frac{d\langle \boldsymbol{x}^2\rangle}{dt} = \gamma_{\boldsymbol{x}}(\langle \boldsymbol{x}\rangle - 2\langle \boldsymbol{x}^2\rangle) + g\left(\overline{\langle \boldsymbol{z}\rangle}, \overline{\langle \boldsymbol{y}\rangle}\right)\overline{\langle \boldsymbol{x}\rangle}\left(\frac{\langle \boldsymbol{x}\rangle}{\overline{\langle \boldsymbol{x}\rangle}} - f\frac{\langle \boldsymbol{z}\rangle - \overline{\langle \boldsymbol{z}\rangle}}{\overline{\langle \boldsymbol{z}\rangle}} + S_{\boldsymbol{x}}\frac{\langle \boldsymbol{y}\rangle - \overline{\langle \boldsymbol{y}\rangle}}{\overline{\langle \boldsymbol{y}\rangle}}\right)$$
$$+ 2g\left(\overline{\langle \boldsymbol{z}\rangle}, \overline{\langle \boldsymbol{y}\rangle}\right)\overline{\langle \boldsymbol{x}\rangle}\left(\frac{\langle \boldsymbol{x}^2\rangle}{\overline{\langle \boldsymbol{x}\rangle}} - f\frac{\langle \boldsymbol{xz}\rangle - \langle \boldsymbol{x}\rangle\overline{\langle \boldsymbol{z}\rangle}}{\overline{\langle \boldsymbol{z}\rangle}} + S_{\boldsymbol{x}}\frac{\langle \boldsymbol{xy}\rangle - \langle \boldsymbol{x}\rangle\overline{\langle \boldsymbol{y}\rangle}}{\overline{\langle \boldsymbol{y}\rangle}}\right) \tag{29}$$
$$\frac{d\langle \boldsymbol{y}^2\rangle}{dt} = \gamma_{\boldsymbol{y}}\left(2\overline{\langle \boldsymbol{y}\rangle}\langle \boldsymbol{y}\rangle - 2\langle \boldsymbol{y}^2\rangle\right) + \sigma_{\boldsymbol{y}}^2 \tag{30}$$
$$\frac{d\langle \boldsymbol{z}^2\rangle}{dt} = \gamma_{\boldsymbol{z}}(\langle \boldsymbol{z}\rangle - 2\langle \boldsymbol{z}^2\rangle) + k_{\boldsymbol{z}}\langle \boldsymbol{x}\rangle + 2k_{\boldsymbol{z}}\langle \boldsymbol{xz}\rangle. \tag{31}$$

Steady-state analysis of this system of differential equations yields the following noise in the cell number

$$CV_{\boldsymbol{x}}^2 = \underbrace{\frac{\gamma_{\boldsymbol{x}}f}{\gamma_{\boldsymbol{z}}\overline{\langle \boldsymbol{z}\rangle}}}_{\substack{\text{Noise from}\\ \text{secreted factor}}} + \underbrace{\frac{\gamma_{\boldsymbol{z}} + \gamma_{\boldsymbol{x}}f}{\gamma_{\boldsymbol{z}}f\overline{\langle \boldsymbol{x}\rangle}}}_{\substack{\text{Noise from}\\ \text{stochastic proliferation}}} + \underbrace{\frac{CV_{\boldsymbol{y}}^2\gamma_{\boldsymbol{x}}S_{\boldsymbol{x}}^2(\gamma_{\boldsymbol{z}}^2 + \gamma_{\boldsymbol{z}}\gamma_{\boldsymbol{y}} + f\gamma_{\boldsymbol{x}}\gamma_{\boldsymbol{y}})}{\gamma_{\boldsymbol{z}}f(\gamma_{\boldsymbol{x}}\gamma_{\boldsymbol{z}}f + \gamma_{\boldsymbol{y}}(\gamma_{\boldsymbol{z}} + \gamma_{\boldsymbol{y}}))}}_{\text{Noise from external disturbance}}. \tag{32}$$

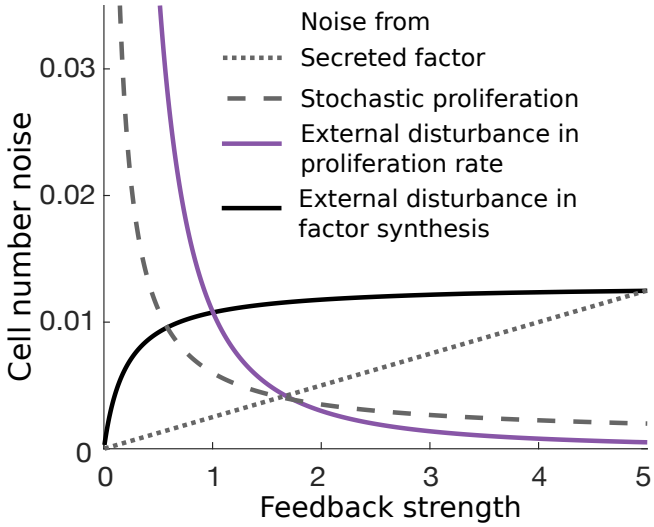

Figure 3: **Depending on the source of noise, random fluctuations in cell numbers can be amplified or buffered with increasing negative feedback strength.** Plots for the noise components shown in (32) and (35) as a function of f. While adding feedback buffers noise from stochastic proliferation and disturbances in the proliferation rate, it amplifies any noise associated with the secreted factor. The latter includes shot noise or Poisson fluctuation in secreted factor copy numbers, and external disturbances to the synthesis rate. Parameters chosen were: $CV_{\boldsymbol{y}}^2 = 0.05, \gamma_{\boldsymbol{z}} = 5\gamma_{\boldsymbol{x}}, \gamma_{\boldsymbol{y}} = \gamma_{\boldsymbol{x}}/5, \overline{\langle \boldsymbol{x} \rangle} = 200, \overline{\langle \boldsymbol{z} \rangle} = 80$.

Comparing with (16) we see an additional third term that represents the contribution from the external disturbance, and this term monotonically decreases to zero as $f \to \infty$ (Fig. 3). Assuming a short-lived secreted factor $\gamma_{\boldsymbol{z}} \gg \gamma_{\boldsymbol{x}}, \gamma_{\boldsymbol{y}}$, (32) reduces to

$$CV_{\boldsymbol{x}}^2 = \underbrace{\frac{\gamma_{\boldsymbol{x}} f}{\gamma_{\boldsymbol{z}} \overline{\langle \boldsymbol{z} \rangle}}}_{\substack{\text{Noise from} \\ \text{secreted factor}}} + \underbrace{\frac{1}{f \overline{\langle \boldsymbol{x} \rangle}}}_{\substack{\text{Noise from} \\ \text{stochastic proliferation}}} + \underbrace{\frac{CV_{\boldsymbol{y}}^2 \gamma_{\boldsymbol{x}} S_{\boldsymbol{x}}^2}{f(\gamma_{\boldsymbol{x}} f + \gamma_{\boldsymbol{y}})}}_{\substack{\text{Noise from} \\ \text{external disturbance}}}. \tag{33}$$

While the noise contribution from stochastic proliferation scales as f^{-1}, depending on the relative values of $\gamma_{\boldsymbol{x}}, \gamma_{\boldsymbol{y}}$ the contribution from external disturbance scales between f^{-1} and f^{-2}. This emphasizes a key point that feedback regulation is more efficient in suppressing noise arising from disturbances in proliferation rate as compared to the inherent stochasticity from small cell numbers. We next consider external disturbance in the synthesis rate $k_{\boldsymbol{z}}$ and revert the proliferation rate back to $g(\boldsymbol{z})$.

4.2 External disturbance in the synthesis rate

The production and secretion of secreted factors is usually mediated by secondary molecules [58], and creates an alternative source of disturbance. To model this feature we modify the factor secretion rate

as $k_{\boldsymbol{z}}(\boldsymbol{y})$, where $\boldsymbol{y}(t)$ is the Ornstein-Uhlenbeck process (19), and as before, linearize the corresponding propensity function

$$k_{\boldsymbol{z}}(\boldsymbol{y})\boldsymbol{x} = k_{\boldsymbol{z}}(\overline{\langle \boldsymbol{y} \rangle})\overline{\langle \boldsymbol{x} \rangle}\left(\frac{\boldsymbol{x}}{\overline{\langle \boldsymbol{x} \rangle}} + S_{\boldsymbol{z}}\frac{\boldsymbol{y} - \overline{\langle \boldsymbol{y} \rangle}}{\overline{\langle \boldsymbol{y} \rangle}}\right), S_{\boldsymbol{z}} := \frac{\overline{\langle \boldsymbol{y} \rangle}}{k_{\boldsymbol{z}}(\overline{\langle \boldsymbol{y} \rangle})}\frac{\partial k_{\boldsymbol{z}}(y)}{\partial y}\bigg|_{y=\overline{\langle \boldsymbol{y} \rangle}}. \tag{34}$$

Here $S_{\boldsymbol{z}}$ is the log sensitivity of the secreted factor synthesis rate to the external disturbance. By performing an analysis similar to the previous section we obtain the following noise in cell numbers

$$CV^2_{\boldsymbol{x}} = \underbrace{\frac{\gamma_{\boldsymbol{x}} f}{\gamma_{\boldsymbol{z}}\overline{\langle \boldsymbol{z} \rangle}}}_{\substack{\text{Noise from} \\ \text{secreted factor}}} + \underbrace{\frac{\gamma_{\boldsymbol{z}} + f\gamma_{\boldsymbol{x}}}{f\gamma_{\boldsymbol{z}}\overline{\langle \boldsymbol{x} \rangle}}}_{\substack{\text{Noise from} \\ \text{stochastic proliferation}}} + \underbrace{\frac{fS^2_{\boldsymbol{z}}CV^2_{\boldsymbol{y}}\gamma_{\boldsymbol{x}}(\gamma_{\boldsymbol{z}} + \gamma_{\boldsymbol{y}})}{f\gamma_{\boldsymbol{x}}\gamma_{\boldsymbol{z}} + \gamma_{\boldsymbol{z}}\gamma_{\boldsymbol{y}} + \gamma^2_{\boldsymbol{y}}}}_{\text{Noise from external disturbance}}, \tag{35}$$

and now the contribution from external disturbance increases with increasing feedback strength f (Fig. 3). This is intuitive, as the disturbance acts through the secreted factor, and adding more feedback only functions to propagate this disturbance to affect cell numbers.

5 Conclusion

How cells regulate their population counts is an intriguing fundamental problem critical for functioning of cellular systems. For example in *Myxococcus xanthus* the formation of fruiting bodies only occurs in presence of precise cell densities and starvation. Further in *Dictyostelium*, during starvation, the cells aggregate to form spores in a fruiting body that is supported by a stalk [59]. If number of spores in the fruiting body are too small, then it will be too close to the ground and cause inefficient spore dispersal. However, if the number of spores is too large then it falls over, possibly ruining a chance of germination of the spores when nutrients become available. We systematically investigated the maintenance of precise cell numbers conferred by a negative feedback mechanism based on extracellular secretion of factors that are sensed by other cells in the population.

While producing low levels of secreted factors may be desirable to minimize energy costs and detection by predators, it comes at the cost of increased biomolecular noise in secreted factor copy numbers. Our analysis shows that while negative feedback suppresses cell number fluctuations from random birth/death of cells, it amplifies fluctuations arising from random birth/death of secreted factors (Fig 2). This results in cell number fluctuations being minimized at an intermediate feedback strength, and a fundamental limit

to noise suppression given by (18). More specifically, the Fano factor (variance/mean or $CV_{\boldsymbol{x}}^2 \times \overline{\langle \boldsymbol{x} \rangle}$) of the cell population count cannot be suppressed beyond $\gamma_x/\gamma_z + 1/\sqrt{N}$. This implies that to have precise control, one not only needs a short-lived factor ($\gamma_x/\gamma_z \ll 1$) but also a high N (average number of factors secreted by an individual cell in its life span). Note that $\gamma_x/\gamma_z \ll 1$ and $N = 4$ gives a Fano factor of one, i.e., the number of cells will have a Poisson distribution, and much larger vales of N would be needed to obtain sub-Poisson statistics. Finally, we mention that similar results have been reported in the context of minimizing protein copy number fluctuations in auto-repressive genetic circuits, where noise sources are differentially effected by negative feedback creating optimal feedback strengths [60–65].

We also considered external disturbances in key model parameters, and depending on where the disturbance enters the systems, it can be amplified or buffered by negative feedback (Fig. 3). While in this work we have focused on a single cell type controlling its numbers, recent experiments reveal communication between different cell types via secreted growth factors to regulate population counts [66]. As part of our future work, we plan to extend the stochastic analysis to a system of multiple cell types interconnected by feedback loops.

Acknowledgment

We thank Dr. Richard Gomer at the Texas A&M University for his helpful feedback on the manuscript. AS is supported by the National Institute of Health Grant 1R01GM126557-01.

References

[1] Roisin-Bouffay C, Gomer RH (2004) How to reach the right size? Med Sci (Paris) 20: 219–224.

[2] Neufeld TP, de la Cruz AFA, Johnston LA, Edgar BA (1998) Coordination of growth and cell division in the drosophila wing. Cell 93: 1183–1193.

[3] Su TT (2000) The regulation of cell growth and proliferation during organogenesis. In Vivo 14: 141–148.

[4] Roisin-Bouffay C, Jang W, Caprette DR, Gomer RH (2000) A precise group size in dictyostelium is generated by a cell-counting factor modulating cell-cell adhesion. Molecular Cell 6: 953–959.

[5] Vargas-Garcia CA, Mohammad S, Singh A (2016) Conditions for cell size homeostasis: A stochastic hybrid systems approach. IEEE Life Sciences Letters 2: 47-50.

[6] Buzi G, Lander AD, Khammash M (2015) Cell lineage branching as a strategy for proliferative control. BMC Biology 13: 13.

[7] Marshall WF, Young KD, Swaffer M, Wood E, Nurse P, et al. (2012) What determines cell size? BMC Biology 10: 101.

[8] Lloyd AC (2013) The Regulation of Cell Size. Cell 154: 1194–1205.

[9] Zaritsky A (2015) Cell-Shape Homeostasis in Escherichia coli Is Driven by Growth, Division, and Nucleoid Complexity. Biophysical Journal 109: 178–181.

[10] Campos M, Surovtsev IV, Kato S, Paintdakhi A, Beltran B, et al. (2014) A constant size extension drives bacterial cell size homeostasis. Cell 159: 1433–1446.

[11] Ghusinga KR, Vargas-Garcia CA, Singh A (2016) A mechanistic stochastic framework for regulating bacterial cell division. Scientific Reports 6: 30229.

[12] Vargas-Garcia CA, Ghusinga KR, Singh A (2018) Cell size control and gene expression homeostasis in single-cells. Current Opinion in Systems Biology 8: 109 - 116.

[13] Singh A, Vargas-Garcia CA, Bjorklund M (2017) Joint regulation of growth and division timing drives size homeostasis in proliferating animal cells. bioRxiv: 173070 .

[14] Vargas-Garcia CA, Soltani M, Singh A (2016) Stochastic hybrid systems approach to modeling dynamics of cell size. IEEE 55th Conference on Decision and Control (CDC) : 5863-5868.

[15] Tzur A, Kafri R, LeBleu VS, Lahav G, Kirschner MW (2009) Cell Growth and Size Homeostasis in Proliferating Animal Cells. Science 325: 167–171.

[16] Turner JJ, Ewald JC, Skotheim JM (2012) Cell Size Control in Yeast. Current Biology 22: R350–R359.

[17] Sauls JT, Li D, Jun S (2016) Adder and a coarse-grained approach to cell size homeostasis in bacteria. Current Opinion in Cell Biology 38: 38–44.

[18] Deforet M, van Ditmarsch D, Xavier JB (2015) Cell-size homeostasis and the incremental rule in a bacterial pathogen. Biophysical Journal 109: 521–528.

[19] Yu FB, Willis L, Chau RMW, Zambon A, Horowitz M, et al. (2017) Long-term microfluidic tracking of coccoid cyanobacterial cells reveals robust control of division timing. BMC Biology 15: 11.

[20] Modi S, Vargas-Garcia CA, Ghusinga KR, Singh A (2017) Analysis of noise mechanisms in cell-size control. Biophysical Journal 112: 2408–2418.

[21] Gomer RH (1997) Cell-density sensing: come on inside and tell us about it. Current Biology 7: R721-2.

[22] Gomer RH (1994) Intercellular signalling. knowing that you're among friends. Current Biology 4: 734–735.

[23] Yuen IS, Gomer RH (1994) Cell density-sensing in dictyostelium by means of the accumulation rate, diffusion coefficient and activity threshold of a protein secreted by starved cells. Journal of Theoretical Biology 167: 273 - 282.

[24] Kim SK, Kaiser D (1990) C-factor: Cell-cell signaling protein required for fruiting body morphogenesis of m. xanthus. Cell 61: 19–26.

[25] Eberhard A (1981) Structural identification of autoinducer of photobacterium fischeri luciferase. Biochemistry 20: 2444–2449.

[26] Grossman AD, Losick R (1988) Extracellular control of spore formation in bacillus subtilis. Proceedings of the National Academy of Sciences 85: 4369–4373.

[27] Gomer RH, Jang W, Brazill D (2011) Cell density sensing and size determination. Development, Growth and Differentiation 53: 482–494.

[28] Brock DA, Hatton RD, Giurgiutiu DV, Scott B, Jang W, et al. (2003) Cf45-1, a secreted protein which participates in dictyostelium group size regulation. Eukaryotic Cell 2: 788–797.

[29] Conlon I, Raff M (1999) Size control in animal development. Cell 96: 235–244.

[30] Thomas M, Langley B, Berry C, Sharma M, Kirk S, et al. (2000) Myostatin, a negative regulator of muscle growth, functions by inhibiting myoblast proliferation. Journal of Biological Chemistry 275: 40235-40243.

[31] Cockcroft CE, den Boer BGW, Healy JMS, Murray JAH (2000) Cyclin d control of growth rate in plants. Nature 405: 575–579.

[32] Choe JM, Bakthavatsalam D, Phillips JE, Gomer RH (2009) Dictyostelium cells bind a secreted autocrine factor that represses cell proliferation. BMC Biochemistry 10: 4.

[33] Suess PM, Gomer RH (2016) Extracellular polyphosphate inhibits proliferation in an autocrine negative feedback loop in dictyostelium discoideum. Journal of Biological Chemistry 291: 20260-20269.

[34] Hespanha JP, Singh A (2005) Stochastic models for chemically reacting systems using polynomial stochastic hybrid systems. International Journal of Robust and Nonlinear Control 15: 669-689.

[35] Singh A, Hespanha JP (2010) Stochastic hybrid systems for studying biochemical processes. Philosophical Transactions of the Royal Society A 368: 4995-5011.

[36] Gillespie DT (1977) Exact stochastic simulation of coupled chemical reactions. Journal of Physical Chemistry 81: 2340–2361.

[37] Singh A, Hespanha JP (2011) Approximate moment dynamics for chemically reacting systems. IEEE Transactions on Automatic Control 56: 414-418.

[38] Chevalier MW, El-Samad H (2011) A data-integrated method for analyzing stochastic biochemical networks. Journal of Chemical Physics 135: 214110.

[39] Lee CH, Kim K, Kim P (2009) A moment closure method for stochastic reaction networks. Journal of Chemical Physics 130: 134107.

[40] Ullah M, Wolkenhauer O (2009) Investigating the two-moment characterisation of subcellular biochemical networks. Journal of Theoretical Biology 260: 340-352.

[41] Gillespie CS (2009) Moment closure approximations for mass-action models. IET Systems Biology 3: 52-58.

[42] Kazeroonian A, Theis FJ, Hasenauero J (2014) Modeling of stochastic biological processes with non-polynomial propensities using non-central conditional moment equation. Proc of the 19th IFAC World Congress, Cape Town, South Africa : 1729–1735.

[43] Soltani M, Vargas-Garcia C, Singh A (2015) Conditional moment closure schemes for studying stochastic dynamics of genetic circuits. IEEE Transactions on Biomedical Systems and Circuits 9: 518-526.

[44] Barzel B, Biham O (2012) Stochastic analysis of complex reaction networks using binomial moment equations. Physical Review E 86: 031126.

[45] Zhang J, Nie Q, Zhou T (2016) A moment-convergence method for stochastic analysis of biochemical reaction networks. The Journal of Chemical Physics 144: 194109.

[46] Smadbeck P, Kaznessis YN (2013) A closure scheme for chemical master equations. PNAS 110: 14261-14265.

[47] Zhang J, DeVille L, Dhople S, Dominguez-Garcia A (2014) A maximum entropy approach to the moment closure problem for stochastic hybrid systems at equilibrium. In: IEEE Conference on Decision and Control. pp. 747-752.

[48] Ghusinga KR, Vargas-Garcia CA, Lamperski A, Singh A (2017) Exact lower and upper bounds on stationary moments in stochastic biochemical systems. Physical Biology 14: 04LT01.

[49] Lamperski A, Ghusinga KR, Singh A (2016) Stochastic optimal control using semidefinite programming for moment dynamics. arXiv:160306309 [mathOC] .

[50] Singh A, Hespanha JP (2006) Stochastic analysis of gene regulatory networks using moment closure. In: Proc. of the 2007 Amer. Control Conference, New York, NY.

[51] Singh A, Hespanha JP (2007) A derivative matching approach to moment closure for the stochastic logistic model. Bulletin of Mathematical Biology 69: 1909-1925.

[52] Kampen NGV (1992) Stochastic Processes in Physics and Chemistry. Amsterdam: North Holland.

[53] Taheri-Araghi S, Bradde S, Sauls JT, Hill NS, Levin PA, et al. (2015) Cell-size control and homeostasis in bacteria. Current Biology 25: 385-391.

[54] Kiviet DJ, Nghe P, Walker N, Boulineau S, Sunderlikova V, et al. (2014) Stochasticity of metabolism and growth at the single-cell level. Nature 514: 376-379.

[55] Ferrezuelo F, Colomina N, Palmisano A, Garí E, Gallego C, et al. (2012) The critical size is set at a single-cell level by growth rate to attain homeostasis and adaptation. Nature Communications 3: 1012.

[56] Hashimoto M, Nozoe T, Nakaoka H, Okura R, Akiyoshi S, et al. (2016) Noise-driven growth rate gain in clonal cellular populations. Proceedings of the National Academy of Sciences 113: 3251-3256.

[57] Lin J, Amir A (2017) The effects of stochasticity at the single-cell level and cell size control on the population growth. Cell Systems 5: 358–367.e4.

[58] Phillips JE, Gomer RH (2014) The p21-activated kinase (pak) family member pakd is required for chemorepulsion and proliferation inhibition by autocrine signals in dictyostelium discoideum. PLoS ONE 9: e96633.

[59] Katoh M, Chen G, Roberge E, Shaulsky G, Kuspa A (2007) Developmental commitment in dictyostelium discoideum. Eukaryotic Cell 6: 2038–2045.

[60] Singh A, Hespanha JP (2009) Optimal feedback strength for noise suppression in autoregulatory gene networks. Biophysical Journal 96: 4013-4023.

[61] Singh A, Hespanha JP (2009) Evolution of gene auto-regulation in the presence of noise. IET Systems Biology 3: 368-378.

[62] Singh A (2011) Negative feedback through mRNA provides the best control of gene-expression noise. IEEE transactions on nanobioscience 10: 194–200.

[63] Dublanche Y, Michalodimitrakis K, Kummerer N, Foglierini M, Serrano L (2006) Noise in transcription negative feedback loops: simulation and experimental analysis. Molecular Systems Biology 2: 41.

[64] Stekel DJ, Jenkins DJ (2008) Strong negative self regulation of prokaryotic transcription factors increases the intrinsic noise of protein expression. BMC Systems Biology .

[65] Singh A (2011) Genetic negative feedback circuits for filtering stochasticity in gene expression. IEEE Conference on Decision and Control, Orlando, FL : 4366–4370.

[66] Zhou X, Franklin RA, Adler M, Jacox JB, Bailis W, et al. (2018) Circuit design features of a stable two-cell system. Cell 172: 744–757.